



Side specific differences of Hounsfield-Units in the osteoporotic lumbar spine

Florian Metzner^{1,2#}, Rebekka Reise^{1,2#}, Christoph-Eckhard Heyde^{1,2}, Nicolas Heinz von der Höh^{2*}, Stefan Schleifenbaum^{1,2*}

¹ZESBO-Center for Research on Musculoskeletal Systems, Faculty of Medicine, Leipzig University, Leipzig, Germany; ²Department of Orthopaedic Surgery, Traumatology and Plastic Surgery, University of Leipzig Medical Center, Leipzig, Germany

Contributions: (I) Conception and design: F Metzner, S Schleifenbaum, CE Heyde; (II) Administrative support: CE Heyde, NH von der Höh; (III) Provision of study materials or patients: CE Heyde, NH von der Höh, S Schleifenbaum; (IV) Collection and assembly of data: R Reise, F Metzner; (V) Data analysis and interpretation: F Metzner, S Schleifenbaum, CE Heyde; (VI) Manuscript writing: All authors; (VII) Final approval of manuscript: All authors.

[#]These authors contributed equally to this work.

^{*}These authors contributed equally to this work as co-senior authors.

Correspondence to: Florian Metzner, M.Sc. Research Associate, ZESBO-Center for Research on Musculoskeletal Systems, Faculty of Medicine, Leipzig University, Semmelweisstraße 14, 04103 Leipzig, Germany; Department of Orthopaedic Surgery, Traumatology and Plastic Surgery, University of Leipzig Medical Center, Leipzig, Germany. Email: florian.metzner@medizin.uni-leipzig.de.

Background: Gold standard for determining bone density as a surrogate parameter of bone quality is measurement of bone mineral density (BMD) by dual energy X-ray absorptiometry (DXA), most commonly performed on the lumbar spine (L1–L4). Computed tomography (CT) data are often available for surgical planning prior to spine procedures, but currently this information is not standardized for bone quality assessment. Besides, measuring the Hounsfield-Units (HU) is also of great importance in the context of biomechanical studies. This *in vitro* study aims in comparing BMD from DXA and HU based on diagnostic CT scans. In addition, methods are presented to quantify local density variations within bones.

Methods: One hundred and seventy-six vertebrae (L1–L4) from 44 body donors (age 84.0±8.7 years) were studied. DXA measurements were obtained on the complete vertebrae to determine BMD, as well as axial CT scans with a slice thickness of 1 mm. Using Mimics Innovation Suite image processing software (Materialise NV, Leuven, Belgium), two volumes (whole vertebra *vs.* spongy bone) were formed for each vertebra, which in turn were divided in their left and right sides. From these total of six volumes, the respective mean HU was determined. HU of the whole vertebra and just spongy HU were compared with the BMD of the corresponding vertebrae. Side specific differences were calculated as relative values.

Results: Whole bone and spongy HU correlated significantly ($P < 0.001$; $\alpha = 0.01$) with BMD. A positive linear correlation was found, which was more pronounced for whole bone HU ($R = 0.72$) than for spongy HU ($R = 0.62$). When comparing the left and right sides within each vertebra, the HU was found to be 10% larger on average on one side compared to the opposite side. In some cases, the difference of left and right spongy bone can be up to 170%. There is a tendency for the side comparison to be larger for the spongy HU than for the whole vertebra.

Conclusions: Determination of HU from clinical CT scans is an important tool for assessing bone quality, primarily by including the cortical portion in the calculation of HU. Unlike BMD, HU can be used to distinguish precisely between individual regions. Some of the very large side-specific gradients of the HU indicate an enormous application potential for preoperative patient-specific planning.

Keywords: Computer tomography (CT); Hounsfield-Units (HU); osteoporosis; vertebral bone; bone quality

Submitted Oct 10, 2023. Accepted for publication Mar 07, 2024. Published online Jun 11, 2024.

doi: 10.21037/jss-23-121

View this article at: <https://dx.doi.org/10.21037/jss-23-121>

Introduction

Dual energy X-ray absorptiometry (DXA) is the gold standard for the diagnosis of osteoporotic bone loss due to its simplicity and low radiation exposure. It usually involves imaging the lumbar spine (L1–L4) as well as the proximal femur in a single plane and calculating the bone mineral density (BMD) projected over the area in g/cm^2 and comparing it with healthy people (T-score). However, when using this method, the diagnosis is often falsely negative due to overestimation of bone mineral content caused by osteophytes, calcification in the surrounding tissue or obesity (1-3). Quantitative computed tomography (QCT) can be performed as an alternative, usually on a single lumbar vertebra (L1–L3). This type of bone density assessment can be performed by using regular computed tomography (CT) equipment. However, a separate scan is necessary in which radiographic phantoms of known radiation absorption are inserted into the scan volume. These phantoms are then used for converting the Hounsfield-Units (HU) into the corresponding mineral density in g/cm^3 (4-6).

CT data of the thoracic or lumbar spine are often available as part of routine examinations such as prior to surgical interventions on the spine. In order to avoid additional radiation exposure due to separate DXA analysis, using clinical CT data for quantifying bone quality is of great interest, especially for surgical planning (7-10). Numerous studies investigated the relationship between HU from clinical spiral CT and the determined BMD or T-score from DXA (3,11-15). Their cut-off values are ranging from 91 to 139 HU for identifying spinal osteoporosis (7,9,11,16-18). HU is thereby usually

measured based on one or more elliptical regions of interest (ROIs) located in the spongy region of lumbar vertebral bodies (2,19,20). Only few studies addressed regional differences within single vertebrae. In these studies, HU was determined either within one or more axial layers within the vertebral body (21) or including the pedicles (22). No significant difference was found between the left and right sides for the entire study group (21). In contrast, Matsukawa *et al.* investigated the HU of multiple volumetric ROIs within individual vertebrae. They focused on the comparison between vertebral bodies and different subregions of the vertebral arch and processes (23).

Biomechanical studies often evaluate different interventions on the spine (implant design, implantation technique) by comparing the left and right sides. This form of study design is a practicable solution due to the limited availability of body donor tissue and its large inter-individual variance (24-30). The results may be influenced by a large side-specific variance in biomechanical properties. This leads to the question of whether side-specific density gradients exist within individual vertebrae and results in three objectives for this study. First, a volumetric approach will be used to determine the vertebral HU with and without the cortical regions. Since cortical areas are included in bone density measurements using DXA, the relationship between BMD and HU will be investigated as well with and without cortical areas. Second, the comparison of volumetric HU determination and previous methods (ellipse in one/three axial slices) will be performed. Finally, the variation of volumetric HU between left and right side within single vertebrae will be investigated. We present this article in accordance with the STROBE reporting checklist (available at <https://jss.amegroups.com/article/view/10.21037/jss-23-121/rc>).

Highlight box

Key findings

- There are side related differences in Hounsfield-Units (HU) within individual lumbar vertebral bones.

What is known and what is new?

- HU of clinical computed tomography (CT) can be used for determination of bone mineral density.
- Side specific differences of HU within lumbar vertebrae were quantified using a volumetric measurement approach.

What is the implication, and what should change now?

- HU of opportunistic CT imaging should be used routinely for qualitative as well as quantitative measure of bone strength.

Methods

Specimen and image acquisition

One hundred and seventy-six vertebrae (L1–L4) from 44 human cadavers (18 females, 26 males) with age of 84.0 ± 8.7 years were obtained in fresh and anatomically unfixed condition and stored at -80°C (Table 1). All body donors gave their informed and written consent to the donation of their bodies for teaching and research purposes while alive. Being part of the body donor program regulated by the Saxonian Death and Funeral Act of 1994 (third section, paragraph 18 item 8), institutional approval for

the use of the post-mortem tissues of human body donors was obtained from the Institute of Anatomy (University of Leipzig) by the Ethics Committee of the University of Leipzig Medical Center (ethical approval No. 129/21-ck). The authors declare that all experiments were conducted according to the principles of the Declaration of Helsinki (as revised in 2013).

CT and DEXA data was gathered from several previous biomechanical studies (27,29). All imaging was conducted on fresh frozen specimen. Each specimen was first subjected

to DXA scanning followed by CT within approximately 2 hours. The following *Table 2* shows the distribution of the human specimens regarding used imaging devices and scan settings. Imaging settings vary due to the absence of specific radiological imaging requirements in some studies. In addition, some studies (27,29) were performed several years apart, which meant that equipment changes or new acquisitions could not be avoided.

Each vertebra was grouped according to its degree of osteoporosis based on DXA as shown in *Table 3*. A large proportion of the body donors exhibited reduced bone quality. Two donors were excluded for HU examination. One had severe degenerative changes which prevented distinguishing the individual vertebrae. The other specimen contained an implant, which resulted in pronounced artifact formation in the CT images. An additional vertebra also had to be excluded due to a pronounced compression fracture.

Table 1 Descriptive statistics regarding the distribution of the individual information of all included donors

Variable	MIN	MAX	Mean	SD
Age (years)	65	98	84.0	8.7
Mass (kg)	30	107	62.3	16.1
Height (cm)	142	176	161	8
BMI (kg/m ²)	13.1	41.3	23.8	5.6

BMI, body mass index; MIN, minimum; MAX, maximum; SD, standard deviation.

Measurement of HU

Mimics Innovation Suite image processing software (Materialise NV, Belgium) was used to mask and semi-

Table 2 Specific clinical scan setting of both DXA and CT imaging

Specification	Study group				
	A (27)	B (29)	C (31)	D (32)	E (32)
CT					
Manufacturer	Philips	Philips	Philips	Philips	Philips
Model	iCT 256	iCT 256	iCT 256	iCT 256	Brilliance Big Bore
Kilovolt peak (kV)	120	120	120	120	120
Tube current (mA)	152	265	152	152	87
Exposure time (mS)	658	755	658	658	2309
Slice thickness (mm)	1	1	1	1	1
Slice spacing (mm)	-1	-1	-0.5	-0.5	-0.5
Pixel spacing (mm)	0.39	0.39	0.39	0.39	0.48
DXA					
Manufacturer	Hologic	Hologic	Hologic	Hologic	Hologic
Model	Delphi A (S/N71109)	Horizon A (S/N303714M)	Delphi A (S/N71109)	Delphi A (S/N71109)	Horizon A (S/N303714M)
Number of donors	10	10	16	5	3
Number of vertebrae	40	40	64	20	12

DXA, dual energy X-ray absorptiometry; CT, computed tomography.

automatically separate the individual vertebral bodies by applying the global thresholding method to the bony parts. Subsequently, the holes inside the vertebrae are closed in order to create a mask that completely fills and represents the bone.

Table 3 Number and relative frequency (%) of all included vertebrae according to their degree of osteoporosis (normal, osteopenic, osteoporotic)

Variable	N	%
Normal	39	22
Osteopenia	54	31
Osteoporosis	83	47
Total	176	100

Classification was based on the T-scores from dual energy X-ray absorptiometry according to the guidelines of the World Health Organization.

The average HU of all voxels within the vertebral bone gives HU_C (Figure 1A). The HU of the spongy bone HU_S (Figure 1B) is defined by uniformly removing about 5 mm from the mask of the complete vertebra using the “Erode” function. This creates a new mask containing only spongy bone regions, thus defining the ROI for determining HU_S . By using the “Crop-Mask” function, the masks HU_C and HU_S are divided into their respective left and right halves (Figure 1C-1E).

Spongy HU is additionally measured using previously published methods to provide a comparison to existing methods. This is done by defining three ellipses (superior, middle, and inferior) in the axial layers of each vertebra. Those ellipses cover the spongy region within the vertebral body, with at least 1 mm distance between the edge of the ellipses and the cortical bone (Figure 2). On one hand, the mean HU of the middle ellipse (HU_m) is determined, and on the other hand, the mean HU from all

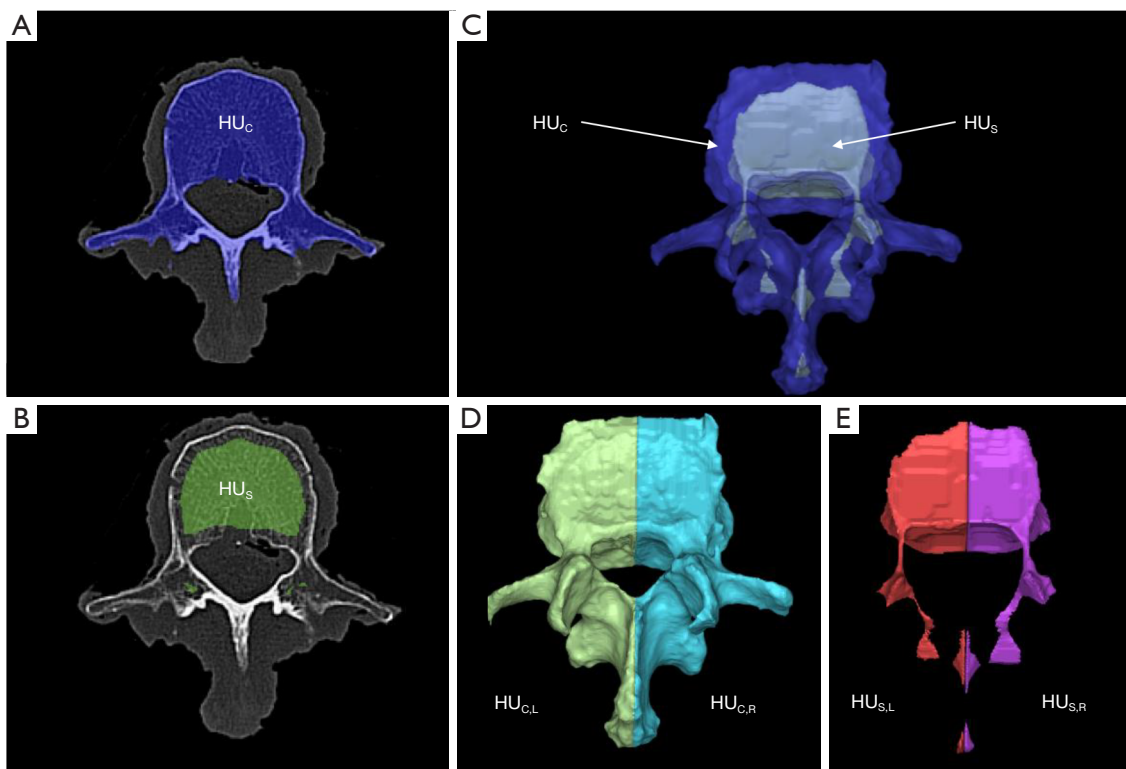


Figure 1 Generation of the volumes as cross-sectional view (A,B) as well as 3D view (C-E). HU_C represents the HU of a complete vertebra including cortical bone and HU_S without cortical bone. $HU_{C,L}$, $HU_{C,R}$, $HU_{S,L}$ and $HU_{S,R}$ show the respective left and right halves of HU_C and HU_S . Outliers of up to 1.5 times the interquartile range are marked as circles. If the factor exceeds 2.5, they are marked with asterisks. This figure is reproduced with kind permission from (32). HU, Hounsfield-Units.

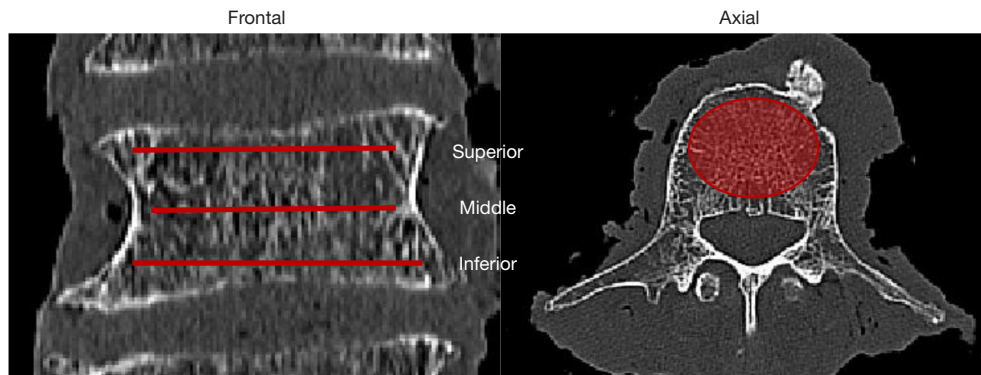


Figure 2 Frontal and axial view of a vertebra with highlighted elliptical regions of interest for evaluating the spongius HU. HU, Hounsfield-Units.

three ellipses (HU_{ave}) of each vertebral body is calculated (2,7,17,33,34).

Both HU_C and HU_S are compared to the BMD of the corresponding vertebrae. Lateral differences are calculated from the left and right partial bodies and expressed as percentages to determine the side-specific differences. Hereafter, this parameter will be referred to as coronal dysbalance (CD). CD is defined by calculating the difference between the left and right HU and relating the difference to the respective lower value. Accordingly, negative numerical values mean higher HU on the right side and vice versa. Furthermore, the absolute value of coronal dysbalance (CD_{AV}) is used to distinguish the extent of CD between individual groups.

Statistical analyses

Descriptive statistics were examined using IBM SPSS Statistics 24 (IBM Corporation, Armonk, NY, USA). Statistical significance is defined with $P < 0.05$. Independent Kruskal-Wallis test was used for comparing group specific differences of HU within the stages of osteoporosis and for comparing the relative differences of side specific HU. Wilcoxon tests were used for testing differences between spongius and cortical HU within the same vertebrae. Spearman correlation as well as simple linear regression was used to determine relationships between BMD and HU_C as well as BMD and HU_S . Bland-Altman plots and linear regressions were used to compare the different methods used to examine the HU within each vertebra (35).

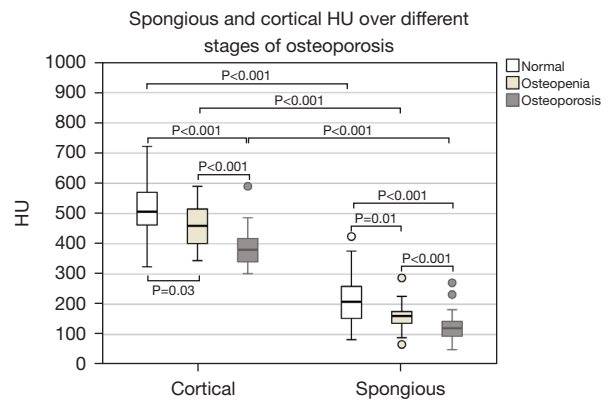


Figure 3 Distribution of cortical and spongius HU grouped by their degree of osteoporosis. HU, Hounsfield-Units.

Results

Distribution of HU regarding osteoporosis

The HU of both vertebral bone (HU_C) and spongius bone (HU_S) are highest in in normal bones, followed by osteopenic and osteoporotic bones. Inter-group differences are consistently significant. HU_C is significantly higher than HU_S among all groups (Figure 3).

HU vs. BMD

There is a significant correlation (Spearman, 2-sided, significance level: 0.01) between BMD and HU_C ($P < 0.001$; $R = 0.724$) as well as between BMD and HU_S ($P < 0.001$;

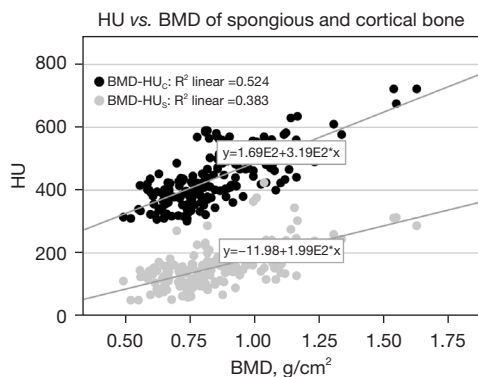


Figure 4 Scatter plots showing the dependence of cortical HU (HU_C) and spongius HU (HU_S) as a function of BMD from DXA analysis. Linear regressions were calculated for each group. HU, Hounsfield-Units; BMD, bone mineral density; DXA, dual energy X-ray absorptiometry.

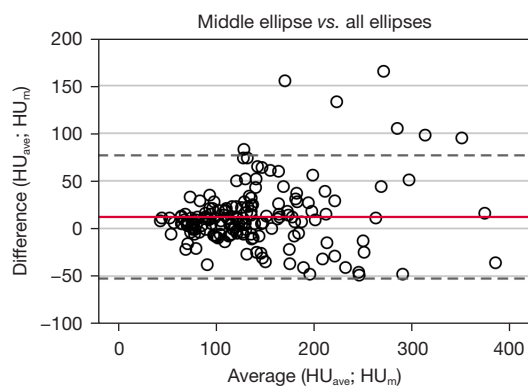


Figure 5 Bland-Altman plot showing the differences of measuring HU via one ellipse and as the average of three ellipses within the vertebral body. The red line indicates the average difference of both measures. HU, Hounsfield-Units.

$R=0.619$). Linear regression analysis also yielded significant results for HU_C over BMD ($P<0.001$; $R^2=0.524$) and HU_S over BMD ($P<0.001$; $R^2=0.383$). A scatter plot with the regression equations is shown in *Figure 4*.

Comparison of HU measurement approaches

Bland-Altman plots and linear regression analyses were performed to compare the outcomes of all HU measurement approaches. First, the results of HU_m and HU_{ave} were compared. The mean difference between

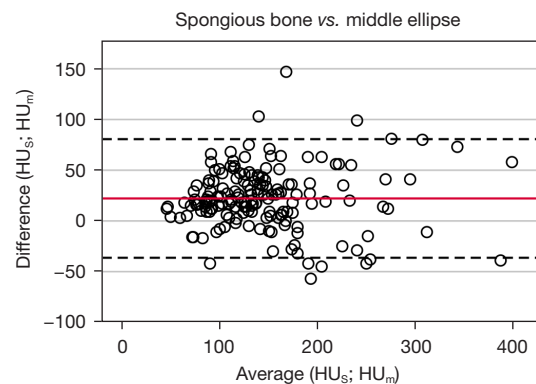


Figure 6 Bland-Altman plot of volumetric spongius HU compared with HU of the central ellipse. The red line indicates the average difference of both measures. HU, Hounsfield-Units.

the measured values is 12.1 ± 33.0 HU. 95.8% of the data points (*Figure 5*) are within the range of variation. Linear regression shows a significant correlation ($P<0.001$, $R^2=0.77$).

The mean difference between HU_S and HU_m is 22.2 ± 29.8 HU (*Figure 6*) and 93.4% of the measured values are within the specified range of variation. A linear regression analysis provides a significant correlation ($P<0.001$, $R^2=0.79$).

Same statistical procedures were used for comparing HU_{ave} and HU_S . The mean difference here is 10.1 ± 21.5 HU and 95.8% of the data points were within the range of variation (*Figure 7*). The linear regression is also significant ($P<0.001$, $R^2=0.90$).

CD (CD , CD_{AV}) of HU

Figure 8 shows the cortical and spongius CD of HU within the vertebra. Again, the groups are classified according to preceding osteoporosis.

No significant differences were found between all groups, but it can be seen that the HU tended to be larger on the right half of the vertebrae than on the left. All examined vertebrae were further categorized to highlight the CD (*Table 4*). Vertebrae in which the CD is less than 5% belong to the “none” category. Remaining vertebrae are classified according to their algebraic sign of relative difference (positive = left, negative = right). The categorization was performed for spongius and cortical bone and is identical in each case. Almost half of the vertebrae thus have higher HU on their right sides.

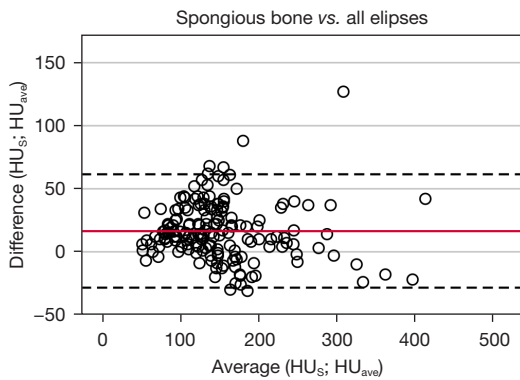


Figure 7 Bland-Altman plot of volumetric spongy HU compared with the HU of all three ellipses. The red line indicates the average difference of both measures. HU, Hounsfield-Units.

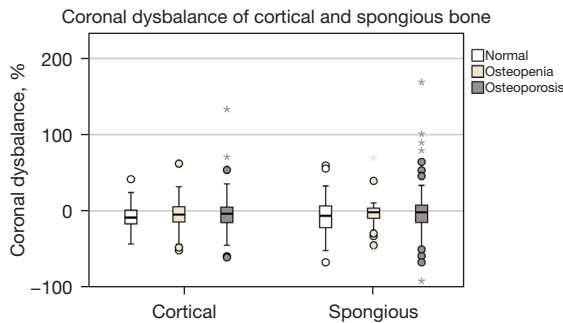


Figure 8 Relative coronal dysbalance of cortical and spongy bone grouped into stages of osteoporosis according to bone mineral density from dual energy X-ray absorptiometry. Positive values resemble higher HU on the left side and vice versa. Outliers of up to 1.5 times the interquartile range are marked as circles. If the factor exceeds 2.5, they are marked with asterisks. HU, Hounsfield-Units.

The extent of CD_{AV} is shown in *Figure 9*. Normal vertebrae show an average of 3.9% higher CD_{AV} in the spongy bone than in the whole vertebra. Maximum values reach up to around 170%. Furthermore, CD_{AV} is significantly lower in osteopenic spongy bone than in normal bone. For whole vertebrae, the median difference in CD_{AV} is $15.4\% \pm 17.2\%$ and for spongy bone $19.3\% \pm 26.0\%$. The detailed results are shown in *Table 5*.

Discussion

The average HU of 176 lumbar vertebrae was examined over the entire bone, the spongy regions as well as their left and right subvolumes. BMD was additionally

Table 4 Number and relative frequency (%) of all included vertebrae according to their CD, which is calculated from the relative difference of the HU in the left and right vertebral halves

Variable	N	%
Left	39	22.2
None	46	26.1
Right	82	46.6
Missing	9	5.1

A vertebra with increased HU on the right side is categorized as “right” and vice versa. Any difference of less than 5% is not assigned to any side (none). Any vertebrae that cannot be evaluated are not included (missing). CD, coronal dysbalance; HU, Hounsfield-Units.

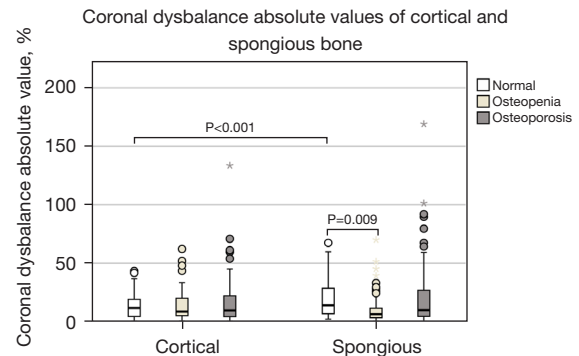


Figure 9 Relative difference values of the coronal dysbalance. Specimens were grouped into normal, osteopenic and osteoporotic as well as into just spongy and cortical bone. Outliers of up to 1.5 times the interquartile range are marked as circles. If the factor exceeds 2.5, they are marked with asterisks.

determined from all vertebrae by DXA and grouped into the corresponding osteoporosis grades (*Table 3*).

Distribution of HU regarding osteoporosis

HU_C is higher than HU_S in osteoporotic, osteopenic and normal vertebrae, which is not surprising since the non-bony components within the interstitial spongy bone are included in the measurement of HU. There are significant differences between the osteoporosis grades for HU_C and HU_S (*Figure 3*). HU_S for osteoporotic, osteopenic, and normal vertebrae are on average 121, 158, and 218 HU, respectively. In this regard, Pinto *et al.* (11) gathered data from eight studies. They showed a range from

Table 5 Detailed results of Hounsfield-Units as well as coronal dysbalance within each vertebra

Variable	Group	Cortical bone						Spongious bone						P
		Mean	Median	SD	SE	P ₅	P ₉₅	Mean	Median	SD	SE	P ₅	P ₉₅	
Volumetric HU	Total	435	420	88	7	317	585	154	143	64	5	71	287	<0.001
	Normal	520	506	88	14	400	722	218	208	82	13	116	376	<0.001
	Osteopenia	459	460	73	10	352	581	158	162	40	6	92	223	<0.001
	Osteoporosis	380	381	49	6	310	442	121	121	38	4	60.5	169	<0.001
CD in %	Total	-4.9	-4.6	22.6	1.7	-40.8	26.1	-2	-3.3	32.4	2.5	-48.7	55.5	0.14
	Normal	-6.5	-8.7	17.1	2.8	-36.6	24.2	-2.4	-6.4	39.5	6.5	-51.9	59.7	0.42
	Osteopenia	-5.3	-4.8	19	2.7	-43.4	22.1	-3.8	-1.6	18.6	2.6	-33	10.4	0.29
	Osteoporosis	-3.9	-3.6	26.7	3	-42.9	30.9	-0.8	-1.6	35.7	4	-49.8	71.9	0.43
CD _{AV} in %	Total	15.4	9.7	17.2	1.3	0.8	47.9	19.3	9.3	26	2	1.3	67.4	0.03
	Normal	13.9	11.6	11.7	1.9	0.3	41.6	24.8	13.9	30.5	5	2.6	67.4	<0.001
	Osteopenia	13.8	8.6	14	2	1.1	47.9	12	6.3	14.6	2.1	1	45.1	0.26
	Osteoporosis	17.1	9.6	20.7	2.3	0.9	59.6	21.3	9.8	28.6	3.2	1.2	84.6	0.09

The statistical differences between the vertebrae including cortical bone and only spongious bone are represented with the corresponding P values. An additional grouping into proceeding osteoporosis, based on DXA imaging, is displayed. HU, Hounsfield-Units; CD, coronal dysbalance; DXA, dual energy X-ray absorptiometry; CD_{AV}, coronal dysbalance absolute value; SD, standard deviation; SE, standard error; P₅, 5% percentile; P₉₅, 95% percentile.

55 to 130 HU for osteoporotic vertebrae, 79 to 146 HU for osteopenic vertebrae, and 121 to 230 HU for normal vertebrae. A cutoff value of approximately 130 to 140 HU can be estimated for HU_S using the boxplots in *Figure 3* to distinguish between osteoporotic and osteopenic vertebrae. Numerous studies have been concerned with the determination of such a threshold (3,7,9,11,36,37). Thresholds of 99 HU (18), 118 HU (19) or 135 HU (17), which are dysbalanced regarding specificity and sensitivity, have been found. The threshold for distinguishing between osteopenia and osteoporosis for HU_C lies about 400 HU. No comparative data were discovered in the literature regarding HU measurements including cortical areas.

HU vs. BMD

Numerous studies have demonstrated a significant correlation between HU from the lumbar vertebrae (L1–L4) and BMD from DXA. Correlation coefficients R compiled by Ahmad *et al.* ranged from 0.46 to 0.76 (3). This compares with the correlation between volumetric determined HU_S with BMD, which provides a moderate correlation (R=0.61). Even higher correlation with (R=0.72) was demonstrated by considering the cortical fractions in

HU_C. The reason for this may be that cortical components are also included in the calculation of the BMD obtained by DXA. Our results thus confirm that when comparing bone density information between CT and DXA, not only the spongious HU within the vertebral body, but also the HU of cortical areas should be included. Bone density assessment from CT images is only practical in a clinical setting, if CT data is already available. Due to higher radiation exposure compared to DXA it might not be a stand-alone diagnostic tool.

Comparison of HU measurement approaches

By comparing the different measurement methods (one ellipse, average of three ellipses, volumetric) it was shown that by evaluating one ellipse within the vertebral body (HU_m) the average values are 22 HU lower than the volumetrically determined HU_S. Thereby, only 93.4% of the data points are within the specified range of fluctuation (*Figure 6*). HU_m and HU_{ave} are on average 12 and 10 HU lower than HU_S and 95.8% of the data points are within the defined fluctuation range. Hence, we conclude that the measurement method must always be considered for a valid use of HU as an instrument for the evaluation of bone

quality. This problem is reflected in the partially different thresholds for distinguishing normal, osteopenic, and osteoporotic bone mentioned above (17-19).

CD (CD, CD_{AV}) of HU

The average CD is -2% for spongiuous bone and -4.9% for cortical bone, whereas negative signs indicate higher values on the right half of the vertebra and vice versa (*Table 5*). In normal bone, CD is slightly greater than in osteopenic and osteoporotic bone, however the differences are not significant. Referring to the classification from *Table 3*, almost half of all vertebrae showed a higher HU on the right side. A possible explanation for this is that there are much more right-handed than left handed individuals. A noticeable aspect of our results is that both the number of outliers and their amounts of about 50% to 170% are higher compared to the other groups, especially within the spongiuous bone of osteoporotic vertebrae (*Table 5*). Moreover, the CD in the spongiuous bone is significantly greater for normal bones than for those involving the cortical bone (*Figure 9*).

Several studies have investigated the variation of HU across different regions within individual vertebrae. Yang *et al.* examined several ROIs (including anterior, left side, right side) from axial slices of 100 lumbar vertebrae and could not find significant differences when comparing the individual regions. However, only the mean or median values of the ROIs over the entire subgroup were compared (21). Odeh *et al.* separated vertebrae into subvolumes (including vertebral body, pedicle, vertebral arch, lateral processes and spinous process) and calculated their bone mineral content from HU using a linear relationship. Cortical (450 < HU < 1,400) and spongiuous (200 < HU < 450) regions were considered separately, but left and right portions (e.g., of the pedicle) were not compared individually (38). Another group around Xu *et al.* determined the mean HU of both pedicles additionally to the HU of the vertebral body. The authors defined elliptical ROI within an axial slice in which both pedicles and the center of the vertebral body can be seen. HU was determined in the pedicle with and without cortical bone, and the mean value was calculated from both the left and right pedicles. Scanning data were then correlated with postoperative pedicle screw loosening. The vertebrae that experienced screw loosening had significantly lower HU in the pedicle as well as the vertebral body (22).

To the best of our knowledge, this is the first study to

investigate and quantify the variation in HU between the left and right sides of the vertebrae. Maximum values of CD_{AV} reach up to 170%. Valuable recommendations for clinical practice could be derived by combining this knowledge with validated thresholds for assessing bone quality from HU. An optimal treatment strategy (e.g., use of bone cement) can thus be derived on a side-specific basis in the case of a large coronal density gradient (9,12,39,40). These data may help to identify an individual approach for an optimal treatment strategy in pedicle screw placement in osteoporotic and osteopenic vertebral bodies in spinal surgery. Several studies investigated to what extent HU can be used for the prediction of screw loosening. They concluded that HU is a better predictor of screw loosening than the DXA T-score, particularly in the lumbar spine (12,40,41). Additional work is still needed regarding the relation between the local HU and implant stability. More valid measurement methods should also be specified for determining threshold values, which can be used for developing optimal recommendations for surgical procedures (36,37). A possible integration of our workflow into clinical practice faces two challenges. One is the reliability of HU itself as a quantitative measure of bone strength. The second problem is developing (semi-) automatic software tools for integrating the presented method into current radiological workflows.

Limitations

Both CT and DEXA scans were performed with frozen spinal specimens. Care was taken when performing DXA scans in order to ensure physiological alignment of the specimens, but there are no influences from surrounding tissues like in situ. The study included CT analyses carried out on different devices. The used scan parameters were listed in *Table 2*. Since all scans used a tube voltage of 120 kV and consistently the same slice thickness, only minor deviations are assumed (36). All scans were done in the same hospital, which means that the scans were performed by the same staff.

No further classification was made of the body donors examined regarding degenerative deformities of the musculoskeletal system. A high average age of the examined donor organs leads to the assumption of a high prevalence of such phenomena.

In the selection of ROIs, no restriction was made regarding blood vessels or degenerative phenomena as was done by other research groups (1,21,22). Local ossifications could thus influence the measurement results. However,

this was partly the aim of the work by pointing out how much the distribution of HU within the vertebral body can differ. The partially large differences might be caused by degenerative phenomena. It is therefore necessary to address the evaluation of such influences in the future.

Conclusions

The determination of bone quality by means of DXA has only limited significance due to the surface projection and is partially prone to errors. Measuring the HU from clinical CT scans, whenever available, enables a general assessment of bone quality using simple analysis methods, although we recommend and see a great potential for standardization of the measurement methods. Furthermore, this study demonstrated that there are sometimes very large CDs in the measured HU within individual vertebrae. These indicate large differences in bone quality. Detailed knowledge of bone density distribution holds enormous potential for preoperative patient-specific planning.

Acknowledgments

Abstract as well as Figure 1 was presented at the 18th Annual Meeting of the German Spine Society (DOI: 10.1007/s00586-023-07991-z). We would like to thank Springer publisher for the permission to publish the abstract and Figure 1. The abstract was also presented in German language at the German Congress of Orthopaedics and Traumatology 2023 (DOI: 10.3205/23dkou306).

Funding: This research was funded by Roland Ernst Stiftung für Gesundheit (Funding Number: ROLAND ERNST STIFTUNG/ 01/21). This article was funded by the Open Access Publishing Fund of Leipzig University, which is supported by the German Research Foundation within the program Open Access Publication Funding.

Footnote

Reporting Checklist: The authors have completed the STROBE reporting checklist. Available at <https://jss.amegroups.com/article/view/10.21037/jss-23-121/rc>

Data Sharing Statement: Available at <https://jss.amegroups.com/article/view/10.21037/jss-23-121/dss>

Peer Review File: Available at <https://jss.amegroups.com/article/view/10.21037/jss-23-121/prf>

Conflicts of Interest: All authors have completed the ICMJE uniform disclosure form (available at <https://jss.amegroups.com/article/view/10.21037/jss-23-121/coif>). The authors have no conflicts of interest to declare.

Ethical Statement: The authors are accountable for all aspects of the work in ensuring that questions related to the accuracy or integrity of any part of the work are appropriately investigated and resolved. All body donors gave their informed and written consent to the donation of their bodies for teaching and research purposes while alive. Being part of the body donor program regulated by the Saxonian Death and Funeral Act of 1994 (third section, paragraph 18 item 8), institutional approval for the use of the post-mortem tissues of human body donors was obtained from the Institute of Anatomy (University of Leipzig) by the Ethics Committee of the University of Leipzig Medical Center (ethical approval No. 129/21-ck). The authors declare that all experiments were conducted according to the principles of the Declaration of Helsinki (as revised in 2013).

Open Access Statement: This is an Open Access article distributed in accordance with the Creative Commons Attribution-NonCommercial-NoDerivs 4.0 International License (CC BY-NC-ND 4.0), which permits the non-commercial replication and distribution of the article with the strict proviso that no changes or edits are made and the original work is properly cited (including links to both the formal publication through the relevant DOI and the license). See: <https://creativecommons.org/licenses/by-nc-nd/4.0/>.

References

1. Carlson BB, Salzmann SN, Shirahata T, et al. Prevalence of osteoporosis and osteopenia diagnosed using quantitative CT in 296 consecutive lumbar fusion patients. *Neurosurg Focus* 2020;49:E5.
2. Schreiber JJ, Anderson PA, Hsu WK. Use of computed tomography for assessing bone mineral density. *Neurosurg Focus* 2014;37:E4.
3. Ahmad A, Crawford CH 3rd, Glassman SD, et al. Correlation between bone density measurements on CT or MRI versus DEXA scan: A systematic review. *N Am Spine Soc J* 2023;14:100204.
4. Adams JE. Quantitative computed tomography. *Eur J Radiol* 2009;71:415-24.
5. Brown JK, Timm W, Bodeen G, et al. Asynchronously

- Calibrated Quantitative Bone Densitometry. *J Clin Densitom* 2017;20:216-25.
6. Lee DC, Hoffmann PF, Kopperdahl DL, et al. Phantomless calibration of CT scans for measurement of BMD and bone strength-Inter-operator reanalysis precision. *Bone* 2017;103:325-33.
 7. Scheyerer MJ, Ullrich B, Osterhoff G, et al. Hounsfield units as a measure of bone density-applications in spine surgery. *Unfallchirurg* 2019;122:654-61.
 8. Meredith DS, Schreiber JJ, Taher F, et al. Lower preoperative Hounsfield unit measurements are associated with adjacent segment fracture after spinal fusion. *Spine (Phila Pa 1976)* 2013;38:415-8.
 9. Zaidi Q, Danisa OA, Cheng W. Measurement Techniques and Utility of Hounsfield Unit Values for Assessment of Bone Quality Prior to Spinal Instrumentation: A Review of Current Literature. *Spine (Phila Pa 1976)* 2019;44:E239-44.
 10. Schwaiger BJ, Gersing AS, Baum T, et al. Bone mineral density values derived from routine lumbar spine multidetector row CT predict osteoporotic vertebral fractures and screw loosening. *AJNR Am J Neuroradiol* 2014;35:1628-33.
 11. Pinto EM, Neves JR, Teixeira A, et al. Efficacy of Hounsfield Units Measured by Lumbar Computer Tomography on Bone Density Assessment: A Systematic Review. *Spine (Phila Pa 1976)* 2022;47:702-10.
 12. Zou D, Sun Z, Zhou S, et al. Hounsfield units value is a better predictor of pedicle screw loosening than the T-score of DXA in patients with lumbar degenerative diseases. *Eur Spine J* 2020;29:1105-11.
 13. Davidson S, Vecellio A, Flagstad I, et al. Discrepancy between DXA and CT-based assessment of spine bone mineral density. *Spine Deform* 2023;11:677-83.
 14. Hendrickson NR, Pickhardt PJ, Del Rio AM, et al. Bone Mineral Density T-Scores Derived from CT Attenuation Numbers (Hounsfield Units): Clinical Utility and Correlation with Dual-energy X-ray Absorptiometry. *Iowa Orthop J* 2018;38:25-31.
 15. Lee S, Chung CK, Oh SH, et al. Correlation between Bone Mineral Density Measured by Dual-Energy X-Ray Absorptiometry and Hounsfield Units Measured by Diagnostic CT in Lumbar Spine. *J Korean Neurosurg Soc* 2013;54:384-9.
 16. Lee SJ, Graffy PM, Zea RD, et al. Future Osteoporotic Fracture Risk Related to Lumbar Vertebral Trabecular Attenuation Measured at Routine Body CT. *J Bone Miner Res* 2018;33:860-7.
 17. Pickhardt PJ, Pooler BD, Lauder T, et al. Opportunistic screening for osteoporosis using abdominal computed tomography scans obtained for other indications. *Ann Intern Med* 2013;158:588-95.
 18. Buckens CF, Dijkhuis G, de Keizer B, et al. Opportunistic screening for osteoporosis on routine computed tomography? An external validation study. *Eur Radiol* 2015;25:2074-9.
 19. Schreiber JJ, Anderson PA, Rosas HG, et al. Hounsfield units for assessing bone mineral density and strength: a tool for osteoporosis management. *J Bone Joint Surg Am* 2011;93:1057-63.
 20. Kim KJ, Kim DH, Lee JI, et al. Hounsfield Units on Lumbar Computed Tomography for Predicting Regional Bone Mineral Density. *Open Med (Wars)* 2019;14:545-51.
 21. Yang G, Wang H, Wu Z, et al. Prediction of osteoporosis and osteopenia by routine computed tomography of the lumbar spine in different regions of interest. *J Orthop Surg Res* 2022;17:454.
 22. Xu F, Zou D, Li W, et al. Hounsfield units of the vertebral body and pedicle as predictors of pedicle screw loosening after degenerative lumbar spine surgery. *Neurosurg Focus* 2020;49:E10.
 23. Matsukawa K, Abe Y, Yanai Y, et al. Regional Hounsfield unit measurement of screw trajectory for predicting pedicle screw fixation using cortical bone trajectory: a retrospective cohort study. *Acta Neurochir (Wien)* 2018;160:405-11.
 24. Brasiliense LB, Lazaro BC, Reyes PM, et al. Characteristics of immediate and fatigue strength of a dual-threaded pedicle screw in cadaveric spines. *Spine J* 2013;13:947-56.
 25. Burval DJ, McLain RF, Milks R, et al. Primary pedicle screw augmentation in osteoporotic lumbar vertebrae: biomechanical analysis of pedicle fixation strength. *Spine (Phila Pa 1976)* 2007;32:1077-83.
 26. Cook SD, Salkeld SL, Stanley T, et al. Biomechanical study of pedicle screw fixation in severely osteoporotic bone. *Spine J* 2004;4:402-8.
 27. Jarvers JS, Schleifenbaum S, Pfeifle C, et al. Comparison of three different screw trajectories in osteoporotic vertebrae: a biomechanical investigation. *BMC Musculoskelet Disord* 2021;22:418.
 28. Paik H, Dmitriev AE, Lehman RA Jr, et al. The biomechanical effect of pedicle screw hubbing on pullout resistance in the thoracic spine. *Spine J* 2012;12:417-24.
 29. Schleifenbaum S, Vogl AC, Heilmann R, et al. Biomechanical comparative study of midline cortical vs.

- traditional pedicle screw trajectory in osteoporotic bone. *BMC Musculoskelet Disord* 2023;24:395.
30. Yüksel KZ, Adams MS, Chamberlain RH, et al. Pullout resistance of thoracic extrapedicular screws used as a salvage procedure. *Spine J* 2007;7:286-91.
 31. Heilmann R, Schleifenbaum S, Heyde CE, et al. 17th German Spine Congress, Annual Meeting of the German Spine Society: P002 Biomechanical analysis of cage movement in 360° fixation during the early postoperative phase with osteoporosis. *Eur Spine J* 2022;31:3201.
 32. Metzner F, Reise R, von der Höh NH, et al. 18th German Spine Congress Annual Meeting of the German Spine Society 29th November to 1st December 2023 Stuttgart, Germany: P 043 A volumetric determination of Hounsfield-Units to identify patient-specific local density differences in osteoporotic lumbar vertebrae. *Eur Spine J* 2024:807.
 33. Pickhardt PJ, Lee LJ, del Rio AM, et al. Simultaneous screening for osteoporosis at CT colonography: bone mineral density assessment using MDCT attenuation techniques compared with the DXA reference standard. *J Bone Miner Res* 2011;26:2194-203.
 34. Romme EA, Murchison JT, Phang KF, et al. Bone attenuation on routine chest CT correlates with bone mineral density on DXA in patients with COPD. *J Bone Miner Res* 2012;27:2338-43.
 35. Bland JM, Altman DG. Statistical methods for assessing agreement between two methods of clinical measurement. *Lancet* 1986;1:307-10.
 36. Lenchik L, Weaver AA, Ward RJ, et al. Opportunistic Screening for Osteoporosis Using Computed Tomography: State of the Art and Argument for Paradigm Shift. *Curr Rheumatol Rep* 2018;20:74.
 37. Shirley M, Wanderman N, Keaveny T, et al. Opportunistic computed tomography and spine surgery: a narrative review. *Global Spine J* 2020;10:919-28.
 38. Odeh K, Rosinski A, Mittal A, et al. Does the Bone Mineral Density of the Lumbar Spine Correlate With Dual-Energy X-ray Absorptiometry T Score? A Cadaveric-Based Analysis of Computed Tomography Densitometry. *Int J Spine Surg* 2023;17:132-8.
 39. Schreiber JJ, Hughes AP, Taher F, et al. An association can be found between hounsfield units and success of lumbar spine fusion. *HSS J* 2014;10:25-9.
 40. Bredow J, Boese CK, Werner CM, et al. Predictive validity of preoperative CT scans and the risk of pedicle screw loosening in spinal surgery. *Arch Orthop Trauma Surg* 2016;136:1063-7.
 41. Lee M, Lee E, Lee JW. Value of computed tomography Hounsfield units in predicting pedicle screw loosening in the thoracic spine. *Sci Rep* 2022;12:18279.

Cite this article as: Metzner F, Reise R, Heyde CE, von der Höh NH, Schleifenbaum S. Side specific differences of Hounsfield-Units in the osteoporotic lumbar spine. *J Spine Surg* 2024;10(2):232-243. doi: 10.21037/jss-23-121